On Impedance Spectroscopy Contribution to Failure Diagnosis in Wind Turbine Generators

Mohamed Becherif[1], El Houssin El Bouchikhi[2] and Mohamed Benbouzid[2]

Abstract – *Wind turbines proliferation in industrial and residential applications is facing the problem of maintenance and fault diagnosis. Periodic maintenances are necessary to ensure an acceptable life span. The aim of this paper is therefore to assess impedance spectroscopy contribution to the failure diagnosis of doubly-fed induction generator-based wind turbines. Indeed, impedance spectroscopy is already used for the diagnosis of batteries, fuel cells, and electrochemical systems. For evaluation purposes, simulations are carried-out on a 9-MW wind farm consisting of six 1.5-MW wind turbines connected to a 25-kV distribution system that exports power to a 120-kV grid. In this context, two common failures are investigated: phase grounding and phase short-circuits. In addition, generator stator resistance variation is also considered for performance evaluation of impedance spectroscopy.*

Keywords*: Wind turbine, doubly-fed induction generator, failure diagnosis, impedance spectroscopy.*

Nomenclature

WT	=	Wind Turbine;
DFIG	=	Doubly-Fed Induction Generator;
IS	=	Impedance Spectroscopy;
E	=	Voltage;
I	=	Current;
Z (*R*)	=	Impedance (Resistance).

I. Introduction

A quantitative analysis of real wind turbine failure data has shown important features of failure rate values and trends. A failures number distribution check-off is reported in Fig. 1 for Swedish, Danish and German wind power plants that occurred between 1994 and 2004 [1]. These figures show that approximately 45% of failures were linked to the electrical system, sensors and blades/pitch components. The experience feedback of wind turbine industries states that the major concern is on the electrical system. Typical failures include: dynamic air gap irregularities, generator bearing failure, stator and rotor winding; insulation failures, inter-turn short circuits in stator windings, broken rotor bar or cracked rotor end-rings and harmonic degrading.

In particular, DFIG-based WT failure diagnosis seems to become an active area of research. Indeed, many papers are devoted to this topic [2-7].

I.1. What about Wind Turbine Failure Diagnosis?

Many techniques and tools have been developed for wind turbine electric generator condition monitoring in order to prolong their life span as discussed in [8].

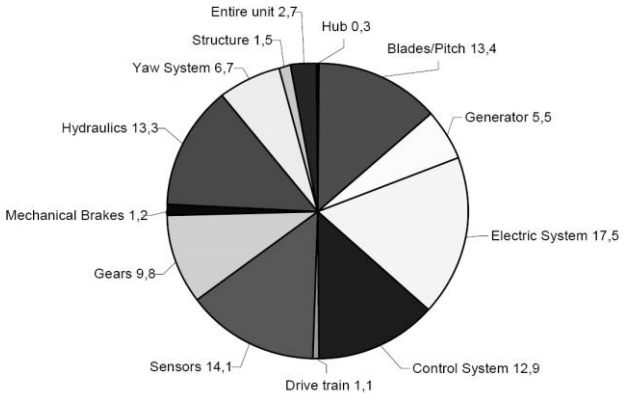

(a) Failures number distribution for Swedish wind power plants (2000-2004).

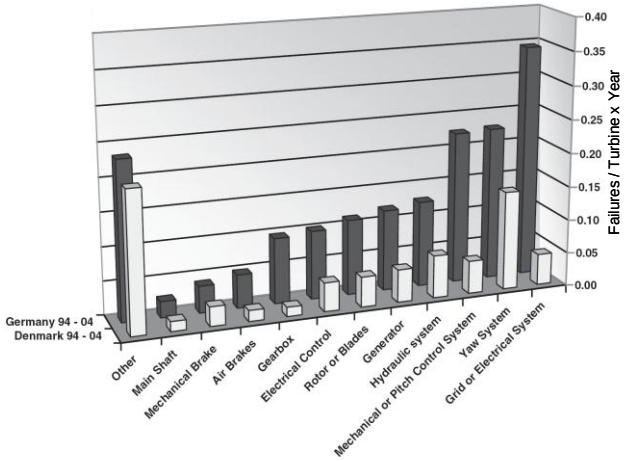

(b) Failure rates for Danish and German wind power plants.

Fig. 1. Wind turbine failure rates [1].

Some of these techniques used the existing and pre-installed sensors, which may measure speed, output torque, vibrations, temperature, flux densities, etc. These sensors are managed together in different architectures and coupled with algorithms to allow an efficient monitoring of the system condition [9]. Those methods have shown their effectiveness in electric motor condition monitoring. From the theoretical and experimental point of view, the well-established methods are: electrical quantities signature analysis (current, power, etc.), vibration monitoring, temperature monitoring and oil monitoring.

In the case of wind turbines, it has been shown that failures in the drive train could be diagnosed from the generator electrical quantities. The advantage of signature analysis of the generator electrical quantities is that those quantities are easily accessible during operation. For steady-state operations, the Fast Fourier Transform (FFT), the PSD (Power Spectral Density) and other techniques based upon them, as for example the STFT (Short-Time Fourier Transform), are widely used in the literature. However, in the case of variable speed offshore wind and marine turbines, FFT is difficult to interpret and it is difficult to extract the variation features in time-domain, since the operation is predominately non stationary due the stochastic behavior of the wind speed. To overcome this problem, advanced signal processing techniques have been proposed. They are compared and evaluated in [4-5].

I.2. What is Specifically Proposed?

The aim of this paper is to evaluate the appropriateness of particular technique that is impedance spectroscopy [10]. Indeed, impedance spectroscopy has already been used for the diagnosis of batteries, fuel cells, and electrochemical systems [11-14]. In this context, IS appears as a promising failure diagnosis technique. It is the method of choice for characterizing the electrical behavior of systems in which the overall behavior is determined by a number of strongly coupled processes.

The current availability of commercially made, high-quality impedance bridges and automatic measuring equipment covering the millihertz to megahertz frequency range is an extra justification to explore IS WTs failure diagnosis. IS should become increasingly popular as more and more engineers understand its theoretical basis and gain skill in the interpretation of impedance data.

I.3.Investigated Failures

Various failures can affect a wind turbine DFIG. In grid codes context, the two frequent failures are phase grounding and phase short-circuits [15]. In addition, DFIG stator resistance variation is also considered for IS diagnosis performance evaluation.

II. Impedance Spectroscopy

II.1. Definitions

Impedance spectroscopy is a general term that subsumes the small-signal measurement of the linear electrical response of a material of interest (including electrode effects) and the subsequent analysis of the response to yield useful information about the physico-electrochemical properties of the system (Fig. 2). Analysis is generally carried-out in the frequency domain, although measurements are sometimes made in the time-domain and then Fourier transformed to the frequency domain, see [16] for an in-depth review.

While

$$R = \frac{E}{I} \tag{1}$$

is a well-known relationship, its use is limited to only one circuit element (the ideal resistor). An ideal resistor has several simplifying properties: It follows Ohm's law at all current and voltage levels; its resistance value is independent of frequency; AC current and voltage signals through a resistor are in phase with each other. Industry applications contain circuit elements with more complex behavior, and then impedance is used instead of resistance. Like resistance, impedance is a measure of the ability of a circuit to resist the flow of electrical current. Unlike resistance, impedance is not limited by the simplifying properties above-listed.

Electrochemical or electrical impedance is usually measured by applying an AC potential to an element and measuring the current through it. Applying a sinusoidal potential excitation leads to an AC current signal response. This current signal can be analyzed as a sum of sinusoidal functions (Fourier series).

Electrochemical impedance is normally measured using a small excitation signal. This is done so that the system response is pseudo-linear. In a linear (or pseudo-linear) system, the current response to a sinusoidal potential will be a sinusoid at the same frequency but phase-shifted (Fig. 2). The excitation signal has the following form

$$E_t = E_0 \sin \omega t \tag{2}$$

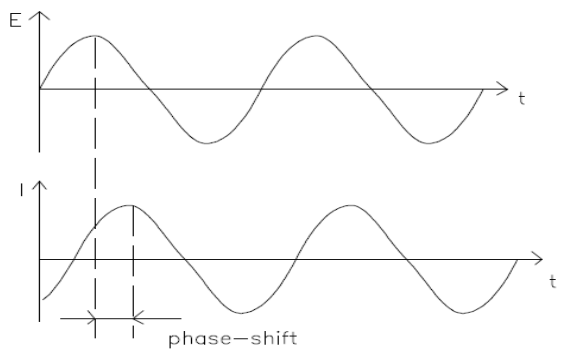

Fig. 2. Sinusoidal current response in a linear system.

In a linear system, the response signal I_t, is phase-shifted and has a different amplitude I_0.

$$I = I_0 \sin(\omega t + \phi) \quad (3)$$

Figure 3 is the Lissajous representation which describes the system complex harmonic motion. When the input to an LTI (Linear Time Invariant) system is sinusoidal, the output is sinusoidal with the same frequency. An LTI system produces an ellipse. The equivalent Nyquist plot is given by Fig. 4 (for a 1st order system).

Using Euler relationship

$$e^{j\phi} = \cos\phi + j\sin\phi,$$

it is possible to express the impedance as a complex function. The potential is described as

$$E_t = E_0 e^{j\omega t} \quad (4)$$

and the current response as

$$I_t = I_0 e^{j\omega t + \phi} \quad (5)$$

The impedance is then represented as a complex number

$$Z(\omega) = \frac{E}{I} = Z_0 e^{j\phi} = Z_0(\cos\phi + j\sin\phi) \quad (6)$$

The impedance is therefore expressed in terms of a magnitude Z_0, and a phase shift ϕ. In Fig. 4, it should be noticed that the *y*-axis is negative and that each point on the Nyquist plot is the impedance at a given frequency.

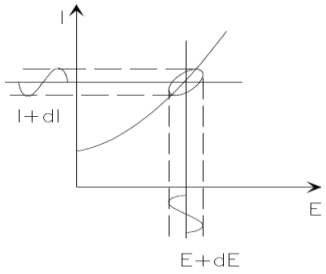

Fig. 3. Lissajous representation.

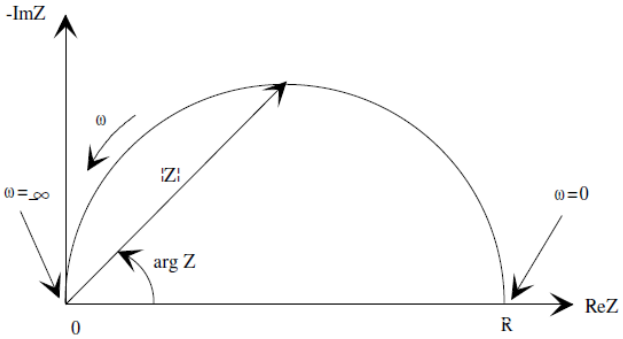

Fig. 4. Nyquist plot with impedance vector.

Low frequency data are on the right-side of the plot and higher ones are on the left-side. On the Nyquist plot, the impedance can be represented as a vector of $|Z_0|$ amplitude. The angle between this vector and the *x*-axis is ϕ (= arg*Z*).

Nyquist plots have one major shortcoming by considering the frequency as an implicit variable.

Data can be plotted either in the frequency- or in time-domain. A transform can be used to switch between the domains. The Fourier transform takes time-domain data and generates the equivalent frequency-domain data.

II.2. Impedance Measurement Process

The impedance measurement entire process is summarized by Fig. 5. It mainly consists in three steps, after measuring the current and the voltage:

1. PWM noise rejection using a sample frequency adjusted to a division of the PWM one. Then the analog-to-digital conversion results in the extraction of desired components of current and voltage ripples.
2. Current and voltage ripples complex expression calculation using a Discrete Fourier Transform (DFT) algorithm that gives measured signals real and imaginary parts. DFT has been adopted to achieve good accuracy even if measured signals exhibit residual perturbation.
3. Spectral impedance computation from the current and voltage, according to the following.

$$Z(f) = Z(j\omega) = \frac{U(j\omega)}{I(j\omega)} = |Z(j\omega)|e^{j\arg[Z(j\omega)]} \quad (7)$$

where $\begin{cases} U(f) = U(j\omega) = |U(j\omega)|e^{j\arg[U(j\omega)]} \\ I(f) = I(j\omega) = |I(j\omega)|e^{j\arg[I(j\omega)]} \end{cases}$

III. Evaluation of the IS-Based Failure Diagnosis Approach

In order to assess impedance spectroscopy contribution to the DFIG-based WT failure diagnosis, a 9-MW wind farm Matlab-Simulink® case study is used for simulation purposes, as illustrated by Fig. 6.

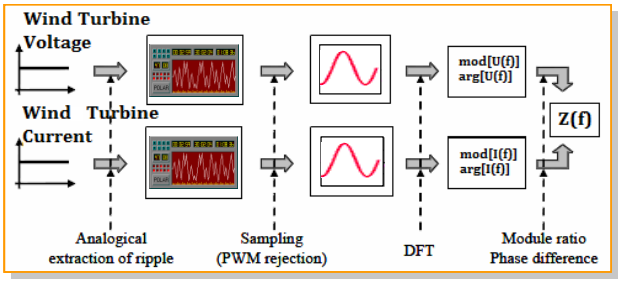

Fig. 5. Impedance measurement process.

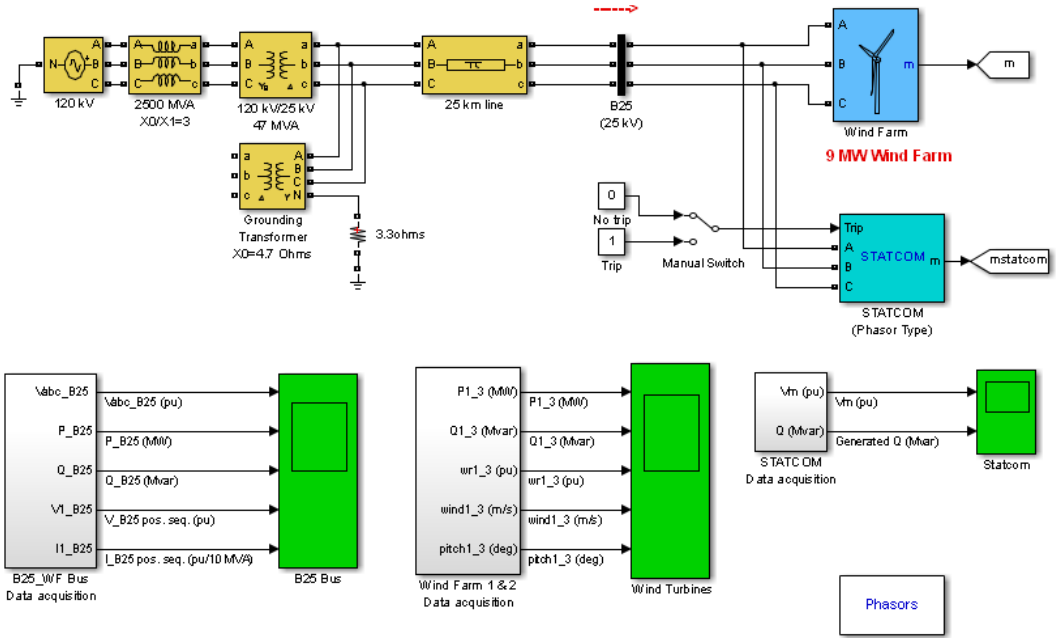

Fig. 6. 9-MW wind farm Matlab-Simulink® case study.

The wind farm consists in six 1.5-MW wind turbines connected to a 25-kV distribution system that exports power to a 120-kV grid through a 30-km, 25-kV feeder. A 500-kW resistive load and a 0.9-MVAR (Q = 50) filter are connected at the 575-V generation bus. Here the wind speed is maintained constant at 10-m/sec. The control system uses a torque controller in order to maintain the speed at 1.09-pu. The reactive power produced by the wind turbine is controlled at 0-MVAR.

The goal is to measure the impedance by applying a single-frequency voltage or current to the studied system. In this case, amplitude and phase-shift (or real and imaginary parts) are measured, using either analog circuit or FFT analysis of the response [17]. As the aim is to focus on the DFIG diagnosis, Figs. 7 and 8, gives respectively the Bode and Nyquist diagrams of a healthy DFIG.

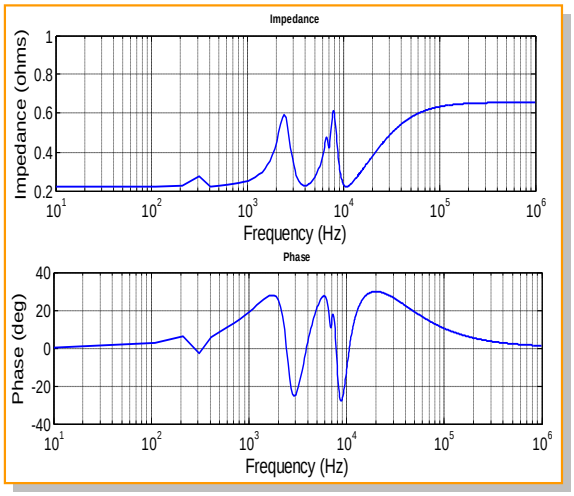

Fig. 7. Bode diagram of a healthy DFIG.

III.1. Phase Grounding Failure

Figures 9 and 10 show phase grounding effects on the measured impedance. As it is expected, the measured impedance is equal to zero (Fig. 10).

III.2. Phase Short-Circuits

In this case, an asymmetrical short-circuit is applied between the DFIG phase A and B. Figure 11 and 12 give respectively Bode and Nyquist impedance plots of phase A (similar results are obtained for phase B).

The faulty curve of Fig. 11 (red dashed line) is below the healthy one as expected. When a short-circuit occurs, the current magnitude increases and consequently the impedance magnitude decreases.

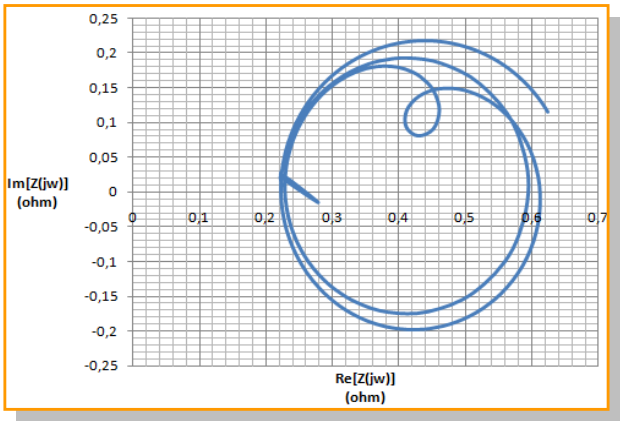

Fig. 8. Nyquist diagram of a healthy DFIG.

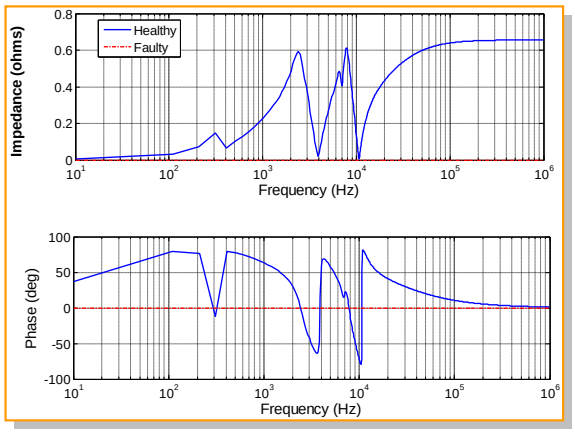

Fig. 9. DFIG Bode diagram with phase grounding.

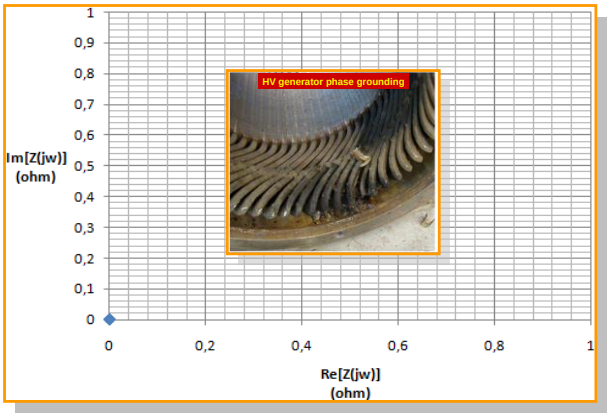

Fig. 10. DFIG Nyquist diagram with phase grounding.

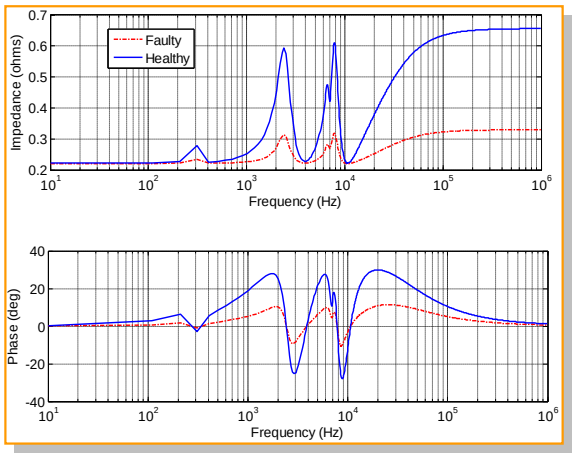

Fig. 11. DFIG Bode diagram with phase short-circuit (between phases A and B).

III.3. DFIG Stator Resistance Variation

A 100% stator resistance increase, which emulates temperature effect, is considered. This particular failure can be easily detected thanks to the DFIG magnitude Bode diagram (Fig. 13). The stator resistance variation induces a constant offset over the whole frequency range. The Nyquist diagram (Fig. 14) shows that the imaginary part of the impedance is equal to that of the healthy DFIG, while the real parts are different.

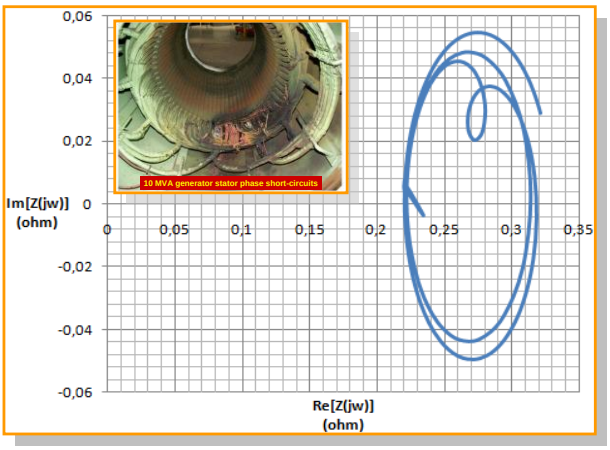

Fig. 12. DFIG Nyquist diagram with phase short-circuit (between phases A and B).

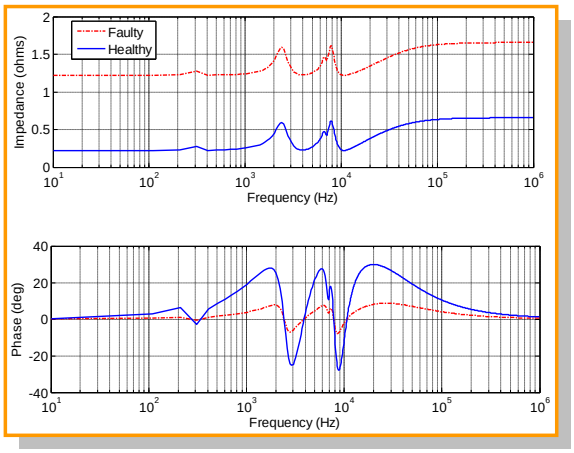

Fig. 13. DFIG Bode diagram with stator resistance variation.

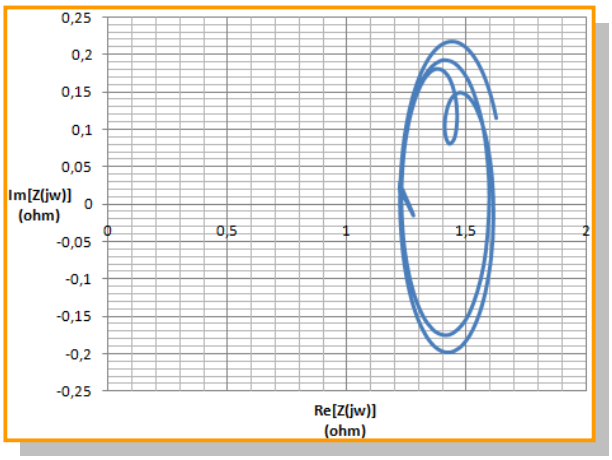

Fig. 14. DFIG Nyquist diagram with stator resistance variation.

This result clearly indicates that parameter variation is a resistance one and not an inductance one.

III.4. What about Failure Diagnosis?

Impedance spectroscopy allows developing a database for a healthy system (generator). A comparison with this

database will therefore lead to failure diagnosis. Indeed, the above-presented failure analysis clearly shows that each failure has its own IS-based signature (impedance) as illustrated by Table 1.

IV. Conclusion

This paper dealt with DFIG-base wind turbine failure diagnosis using impedance spectroscopy. This is a first attempt to evaluate impedance spectroscopy failure diagnosis performance. For evaluation purposes, simulations where carried-out on a 9-MW wind farm consisting of six 1.5-MW wind turbines. In this context, two common failures were investigated: phase grounding and phase short-circuits. In addition, generator stator resistance variation where also considered for performance evaluation of impedance spectroscopy. Failure characteristic Bode and Nyquist diagrams have shown that impedance spectroscopy allows having typical signatures and could be considered as a promising failure diagnosis tool.

References

[1] Y. Amirat, M. Benbouzid, E. Al-Ahmar, B. Bensaker, and S. Turri, "A brief status on condition monitoring and fault diagnosis in wind energy conversion systems," *Renewable and Sustainable Energy Reviews*, vol. 13, no. 9, pp. 2629–2636, 2009.

[2] D.G. Giaourakis, A. Safacas and S. Tsotoulidis, "Fault diagnostic method for open circuit of IGBT converter in doubly-fed induction generator wind energy conversion system," *International Journal on Energy Conversion*, vol. 1, n°1, March 2013.

[3] Y. Amirat, V. Choqueuse, M.E.H. Benbouzid and S. Turri, "Hilbert transform-based bearing failure detection in DFIG-based wind turbines," *International Review of Electrical Engineering*, vol. 6, n°3, pp. 1249-1256, June 2011.

[4] Y. Amirat, V. Choqueuse and M.E.H. Benbouzid, "EEMD-based wind turbine bearing failure detection using the generator stator current homopolar component," *Mechanical Systems and Signal Processing*, vol. 39, n°3, 2013.

Table1. IS-based failure signature (impedance).

	Frequency	Mono-phase	Bi-phase	Tri-phase
	1	2	3	4
1	10.0000 + 0.0000i	0.0029 + 0.0022i	0.0038 + 0.0029i	0.2217 + 0.0010i
2	1.1000e+02 + 0.00...	0.0042 + 0.0250i	0.0064 + 0.0330i	0.2222 + 0.0112i
3	2.1000e+02 + 0.00...	0.0104 + 0.0544i	0.0175 + 0.0707i	0.2244 + 0.0244i
4	3.1000e+02 + 0.00...	0.1211 - 0.0287i	0.1459 - 0.0314i	0.2775 - 0.0145i
5	4.1000e+02 + 0.00...	0.0071 + 0.0487i	0.0125 + 0.0638i	0.2230 + 0.0218i
6	5.1000e+02 + 0.00...	0.0118 + 0.0769i	0.0229 + 0.0992i	0.2243 + 0.0345i
7	6.1000e+02 + 0.00...	0.0180 + 0.0987i	0.0353 + 0.1250i	0.2263 + 0.0446i
8	7.1000e+02 + 0.00...	0.0256 + 0.1190i	0.0493 + 0.1476i	0.2287 + 0.0541i
9	8.1000e+02 + 0.00...	0.0346 + 0.1387i	0.0652 + 0.1681i	0.2316 + 0.0635i
10	9.1000e+02 + 0.00...	0.0453 + 0.1582i	0.0830 + 0.1868i	0.2351 + 0.0732i
11	1.0100e+03 + 0.00...	0.0580 + 0.1778i	0.1025 + 0.2039i	0.2393 + 0.0831i
12	1.1100e+03 + 0.00...	0.0730 + 0.1972i	0.1239 + 0.2193i	0.2445 + 0.0935i
13	1.2100e+03 + 0.00...	0.0907 + 0.2166i	0.1470 + 0.2329i	0.2507 + 0.1044i
14	1.3100e+03 + 0.00...	0.1116 + 0.2357i	0.1721 + 0.2447i	0.2584 + 0.1158i
15	1.4100e+03 + 0.00...	0.1363 + 0.2541i	0.1991 + 0.2544i	0.2679 + 0.1278i
16	1.5100e+03 + 0.00...	0.1656 + 0.2713i	0.2283 + 0.2620i	0.2797 + 0.1404i
17	1.6100e+03 + 0.00...	0.2002 + 0.2864i	0.2599 + 0.2671i	0.2947 + 0.1535i
18	1.7100e+03 + 0.00...	0.2411 + 0.2979i	0.2944 + 0.2693i	0.3139 + 0.1667i
19	1.8100e+03 + 0.00...	0.2889 + 0.3037i	0.3324 + 0.2679i	0.3386 + 0.1792i
20	1.9100e+03 + 0.00...	0.3440 + 0.3006i	0.3747 + 0.2613i	0.3707 + 0.1892i
21	2.0100e+03 + 0.00...	0.4054 + 0.2843i	0.4222 + 0.2470i	0.4120 + 0.1933i
22	2.1100e+03 + 0.00...	0.4696 + 0.2495i	0.4747 + 0.2203i	0.4633 + 0.1853i
23	2.2100e+03 + 0.00...	0.5297 + 0.1917i	0.5289 + 0.1745i	0.5211 + 0.1559i
24	2.3100e+03 + 0.00...	0.5743 + 0.1097i	0.5740 + 0.1032i	0.5722 + 0.0960i

[5] E.H. El Bouchikhi, V. Choqueuse, M.E.H. Benbouzid and J.F Charpentier, "Induction generator-based wind and marines turbines failure diagnosis: Non-stationary signal processing techniques comparative study," *European Journal of Electrical Engineering*, vol. 16, n°3, 2013.

[6] K. Rothenhagen and F.W. Fuchs, "Current sensor fault detection, isolation, and reconfiguration for doubly fed induction generators," *IEEE Trans. Industrial Electronics*, vol. 56, n°10, pp. 4239-4245, October 2009.

[7] E. Al-Ahmar, M.E.H. Benbouzid and S. Turri, "Wind energy conversion systems fault diagnosis using wavelet analysis," *International Review of Electrical Engineering*, vol. 3, n°4, pp. 646-652, July-August 2008.

[8] B. Lu, Y. Li, X. Wu and Z. Yang, "A review of recent advances in wind turbine condition monitoring and fault diagnosis", *in Proceedings of the 2009 IEEE PEMWA*, Lincoln (USA), pp. 1-7, June 2009.

[9] W. Yang, P.J. Tavner, C.J. Crabtree and M. Wilkinson, "Cost-effective condition monitoring for wind turbines," *IEEE Trans. Industrial Electronics*, vol. 57, n°1, pp. 263-271, January 2010.

[10] M. Becherif, A. Henni, M.E.H. Benbouzid and M. Wack, "Impedance spectroscopy failure diagnosis of a DFIG-based wind turbine," *in Proceedings of the 2012 IEEE IECON*, Montreal (Canada), pp. 4310-4315, October 2012.

[11] S.M. Rezaei Niya and M. Hoorfar, "Study of proton exchange membrane fuel cells using electrochemical impedance spectroscopy technique – A review," *Journal of Power Sources*, vol. 240, pp. 281-293, October 2013.

[12] T.C. Kaypmaz and R.N. Tuncay, "An advanced cell model for diagnosing faults in operation of Li-ion Polymer batteries," *in Proceedings of the 2011 IEEE VPPC*, Chicago (USA), pp. 1-5, September 2011.

[13] S. Wasterlain, D. Candusso, F. Harel, X. François and D. Hissel, "Diagnosis of a fuel cell stack using electrochemical impedance spectroscopy and Bayesian networks," *in Proceedings of the 2010 IEEE VPPC*, Lille (France), pp. 1-6, September 2010.

[14] X. Yuan, H. Wang, J.C. Sun and J. Zhang, "AC impedance technique in PEM fuel cell diagnosis – A review," *International Journal of Hydrogen Energy*, vol. 32, n°17, pp. 4365-4380, December 2007.

[15] M. Tsili and S. Papathanassiou, "A review of grid code technical requirements for wind farms," *IET Renewable Power Generation*, vol. 3, n°3, pp. 308-332, September 2009.

[16] E. Barsoukov and J.R. Macdonald, *Impedance Spectroscopy: Theory, Experiment, and Application*. Wiley Interscience Publications, 2005.

[17] M.J. Given, R.A. Fouracre, S.J. MacGregor, M. Judd and H.M. Banford, "Diagnostic dielectric spectroscopy methods applied to water-treed cable," *IEEE Trans. Dielectrics and Electrical Insulation*, vol. 8, n°6, pp. 917-920, December 2001.

[1]UTBM University , FCLab FR CNRS 3539, FEMTO-ST UMR CNRS 6174, 90010 Belfort, France (email: Mohamed.Becherif@utbm.fr).

[2]University of Brest, EA 4325 LBMS, Rue de Kergoat, CS 93837, 29238 Brest Cedex 03, France (e-mail: ElMohamed.Benbouzid@univ-brest.fr).

Mohamed Becherif obtained his B.Sc. degree in control engineering from the Ecole Nationale Polytechnique, Algiers, Algeria, the M.Sc. degree in electrical engineering from the University of Paris-Sud, Paris, France, and the Ph.D. degree in control engineering from the University of Paris-Sud, Paris, France, in 1999, 2001 and 2004, respectively. He received the Habilitation à Diriger des Recherches degree University of Technology of Belfort-Montbéliard, Belfort, France, in 2011.

He was a Lecturer at the University of Paris-Sud, Paris, France from 2004 to 2005. Then, he joined the University of Technology of Belfort-Montbéliard, Belfort, France since 2005, where he is an Associate Professor. His research interests are in the fields of modeling, nonlinear control and energy management of hybrid and renewable systems, with special emphasis on applications.

El Houssin El Bouchikhi was born in Khemisset, Morocco, in 1987. He received the M.Sc. degree in automatic and electrical engineering, from the National Polytechnic Institute of Toulouse, Toulouse, France, in 2010. He is currently working toward the Ph.D. degree on offshore wind and marine current turbines condition monitoring with the University of Brest, Brest, France.

His current research interests are electrical machines fault detection and diagnosis through electrical quantities, especially in non-stationary operating conditions.

Mohamed El Hachemi Benbouzid was born in Batna, Algeria, in 1968. He received the B.Sc. degree in electrical engineering from the University of Batna, Batna, Algeria, in 1990, the M.Sc. and Ph.D. degrees in electrical and computer engineering from the National Polytechnic Institute of Grenoble, Grenoble, France, in 1991 and 1994, respectively, and the Habilitation à Diriger des Recherches degree from the University of Picardie "Jules Verne," Amiens, France, in 2000.

After receiving the Ph.D. degree, he joined the Professional Institute of Amiens, University of Picardie "Jules Verne," where he was an Associate Professor of electrical and computer engineering. Since September 2004, he has been with the Institut Universitaire de Technologie of Brest, University of Brest, Brest, France, where he is a Professor of electrical engineering. His main research interests and experience include analysis, design, and control of electric machines, variable-speed drives for traction, propulsion, and renewable energy applications, and fault diagnosis of electric machines.

Prof. Benbouzid is an IEEE Senior Member. He is the Editor-in-Chief of the International Journal on Energy Conversion (IRECON). He is also an Associate Editor of the IEEE TRANSACTIONS ON ENERGY CONVERSION, the IEEE TRANSACTIONS ON INDUSTRIAL ELECTRONICS, the IEEE TRANSACTIONS ON SUSTAINABLE ENERGY, and the IEEE TRANSACTIONS ON VEHICULAR TECHNOLOGY. He was an Associate Editor of the IEEE/ASME TRANSACTIONS ON MECHATRONICS from 2006 to 2009.